

Synthesis, Spectroscopic Findings, Crystal Engineering of Pb(II)-Salen Coordination Polymers, and Supramolecular Architectures Engineered by σ -hole/Spodium/Tetrel bonds: A Combined Experimental and Theoretical Investigations

Dhrubajyoti Majumdar ^{a*,b}, A. Frontera ^c, Rosa M. Gomila ^c, Sourav Das ^d, Kalipada Bankura^a

^aDepartment of Chemistry, Tamralipta Mahavidyalaya, Tamluk 721636, West Bengal, India

^bDepartment of Chemistry, Indian Institute of Technology (Indian School of Mines), Dhanbad, Jharkhand 826004, India

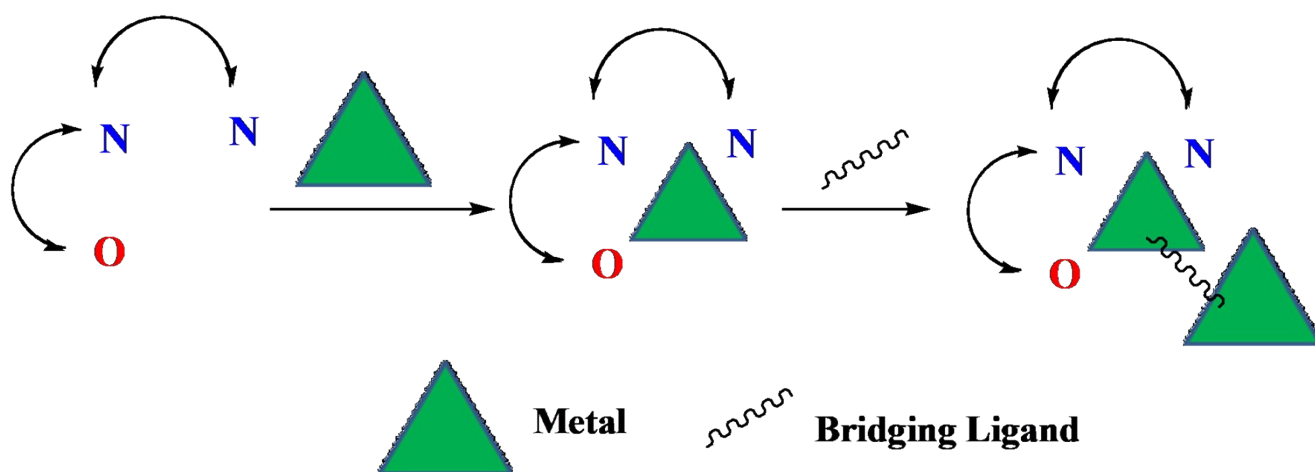
^cDepartment de Química, Universitat de les Illes Balears, Cra. de Valldemossa km 7.5. 07122 Palma de Mallorca (Balears), Spain

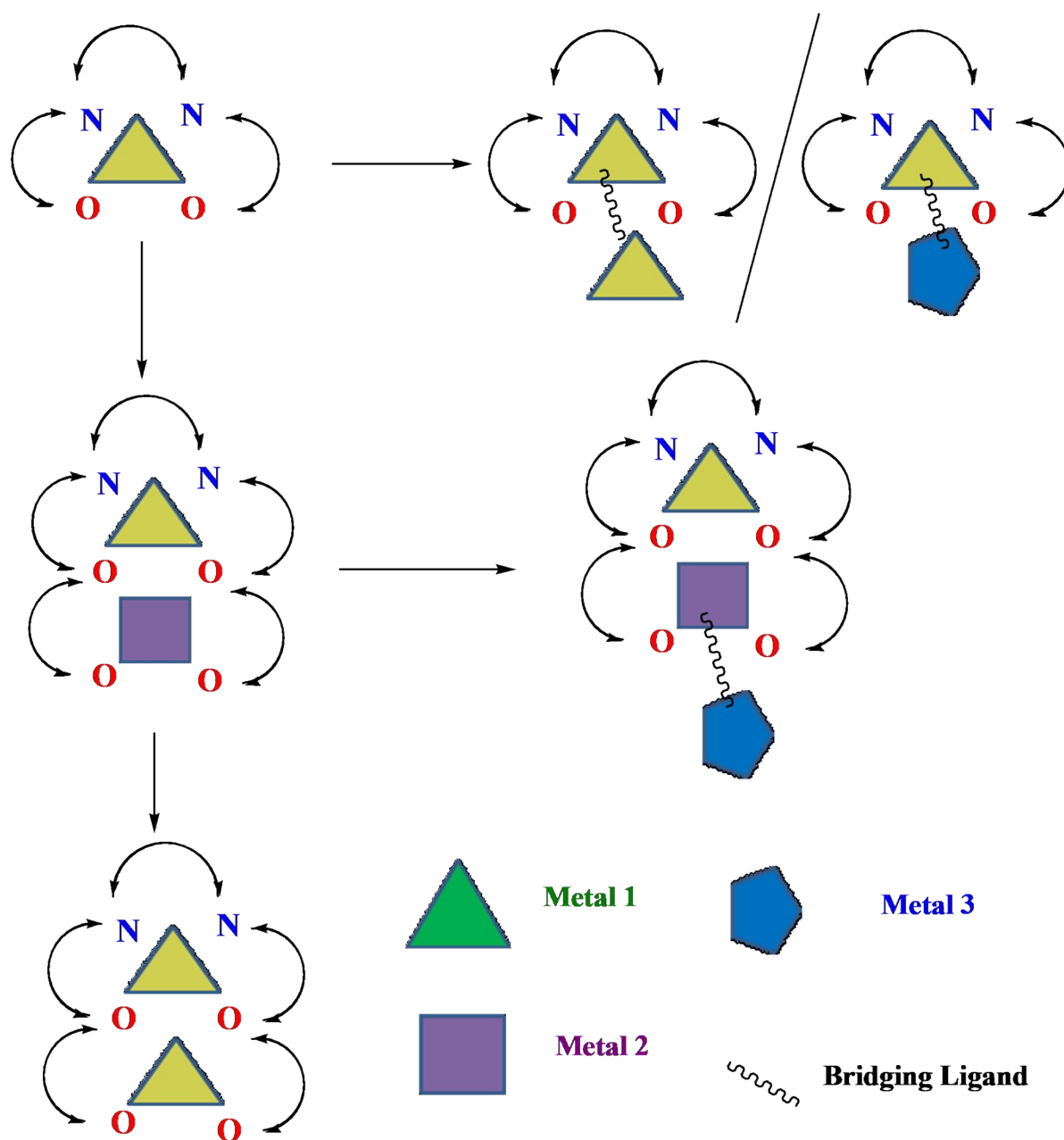
^dDepartment of Basic Sciences, Chemistry Discipline; Institute of Infrastructure Technology Research and Management; Near Khokhara Circle, Maninagar East, Ahmedabad-380026, Gujarat, India

CORRESPONDING AUTHOR EMAIL: dmajumdar30@gmail.com

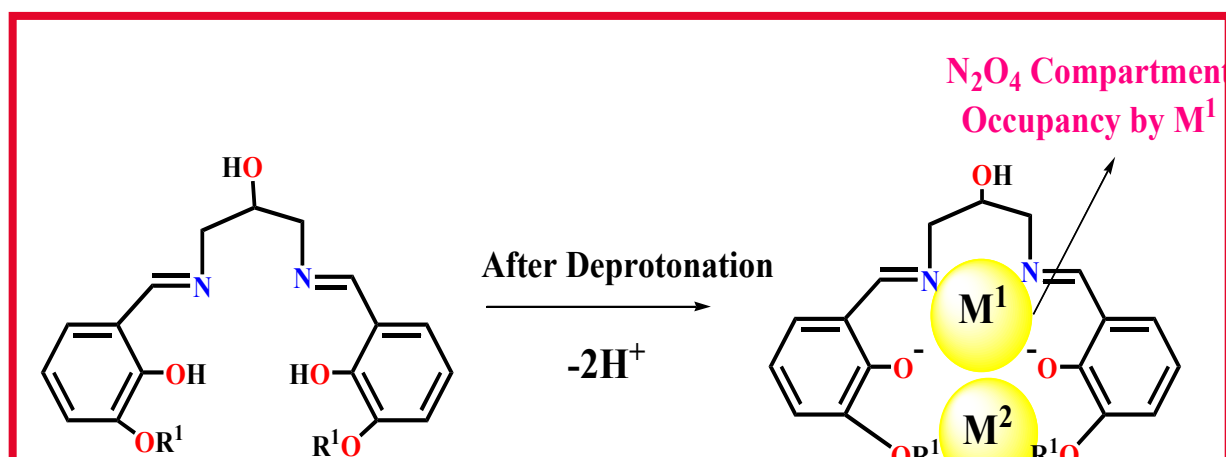
Captions	Schemes/Tables/Figures
Generation of polymeric complexes in the presence of pseudohalides bridging ligand.	Scheme S1
Salen ligand (H ₃ L) compartment mobility (N ₂ O ₂ vs O ₄) with M ²⁺ metal ion.	Scheme S2A

Salen ligands (H_2L^1/H_2L^2) with different nature (M/M^1) metal ions occupancy led to heteronuclear complex formation.	Scheme S2B
Salen ligand (H_3L) compartment occupancy by different metal ions (M^1/M^2) facilitated the heteronuclear complex formation.	Scheme S2C
The simplified Holo-/Hemi-directed coordination spheres around the Pb(II) metal ion.	Scheme S3
NMR proton numbering Scheme of H_3L .	Scheme S4
Coordination polyhedral in Pb(II) complexes with donor ligands.	Scheme S5
Selected important bond distances (\AA) and Bond angles ($^\circ$) for the heteronuclear CP.	Table S1
Reported X-ray characterized Holo-/Hemi-directed heteronuclear Pb(II) complexes.	Table S2
Reported Covalent and Tetrel bond lengths (\AA) in the structures of Pb(II) complexes.	Table S3
MALDI-TOF Mass of the CP	Fig.S1
Representative FT-IR spectra for Salen ligand and CP.	Fig.S1A
Representative Raman spectra for the CP.	Fig.S2
Representative UV-Vis spectra for Salen ligand.	Fig.S3
Representative UV-Vis spectra for CP	Fig.S4
Representative 1H NMR spectra for Salen ligand.	Fig.S5
Representative ^{13}C NMR spectra for Salen ligand.	Fig.S6
Representative 1H NMR spectra for the CP.	Fig.S7
Representative PXRD pattern for the CP	Fig.S8
The perspective view of the asymmetric unit of the CP.	Fig.S9
Histogram plots of Cd-NC (left) and Cd-SC (right) angles in Cd-NCS and Cd-SCN complexes.	

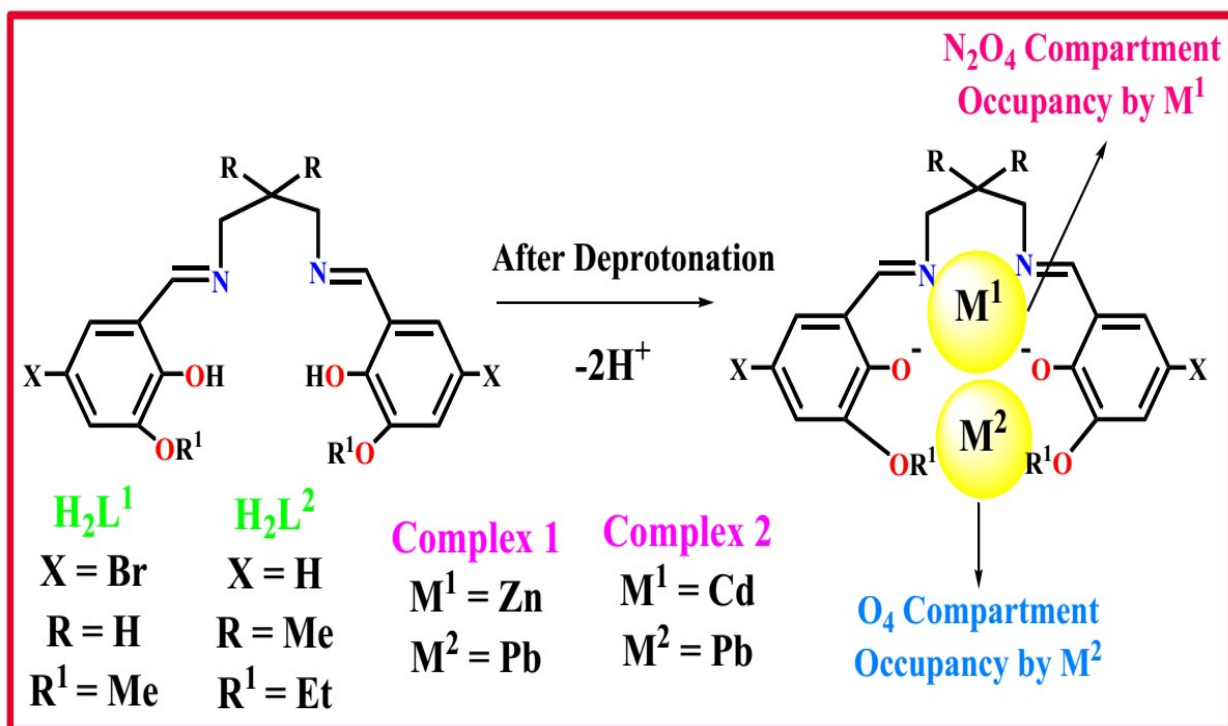




Scheme S1. Generation of polynuclear complexes in the presence of pseudohalides bridging ligand.

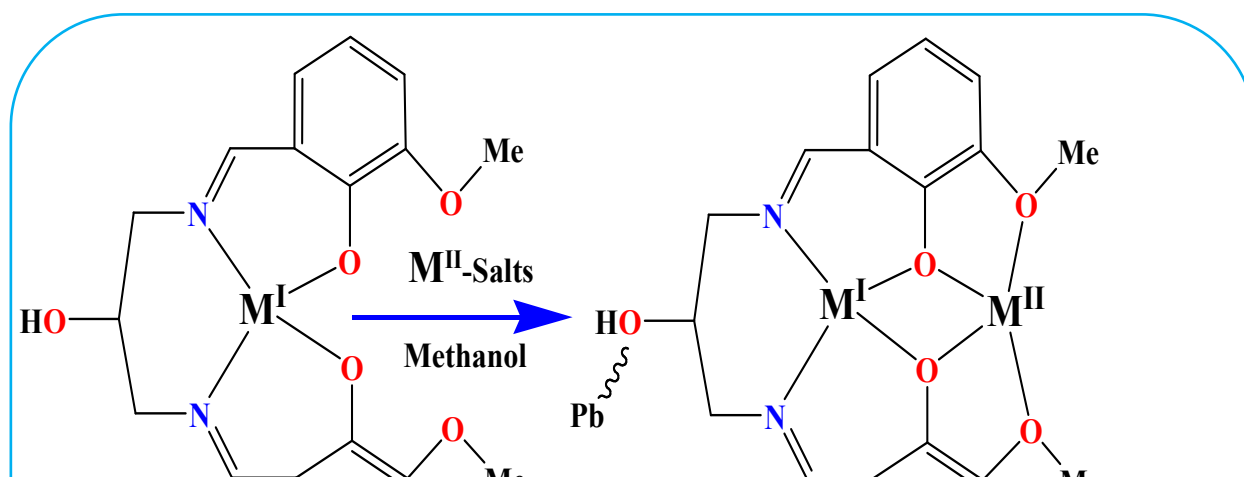


Scheme S2A. Salen (H_3L) compartment mobility (N_2O_2 vs O_4) with M^{2+} metal ion.

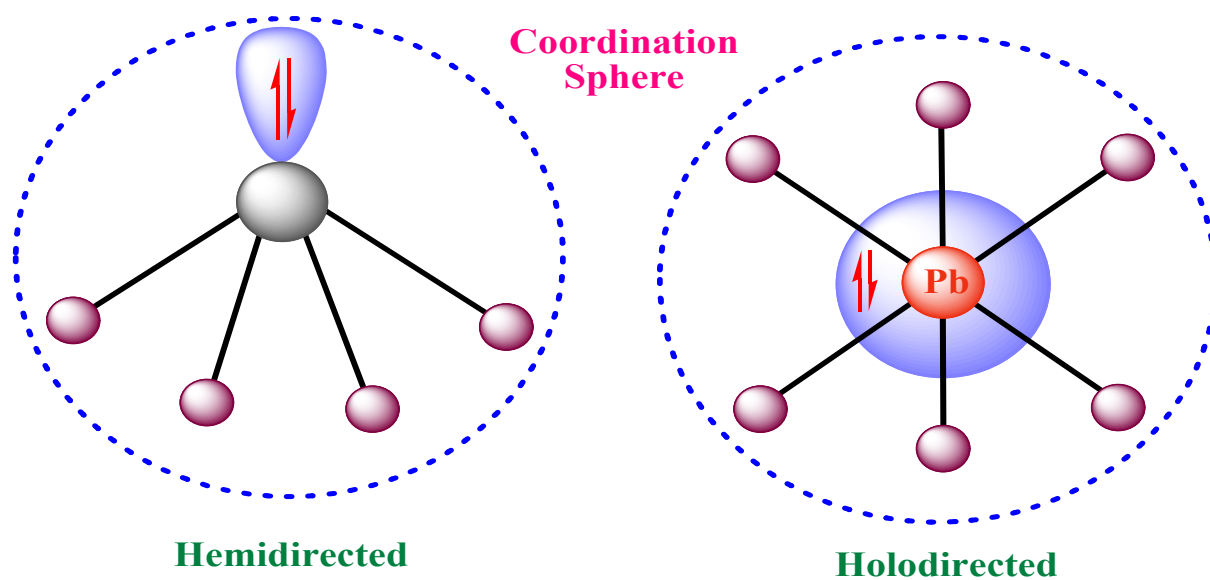


Scheme S2B. Salen ligands (H_2L^1/H_2L^2) compartment occupancy by different metal ions

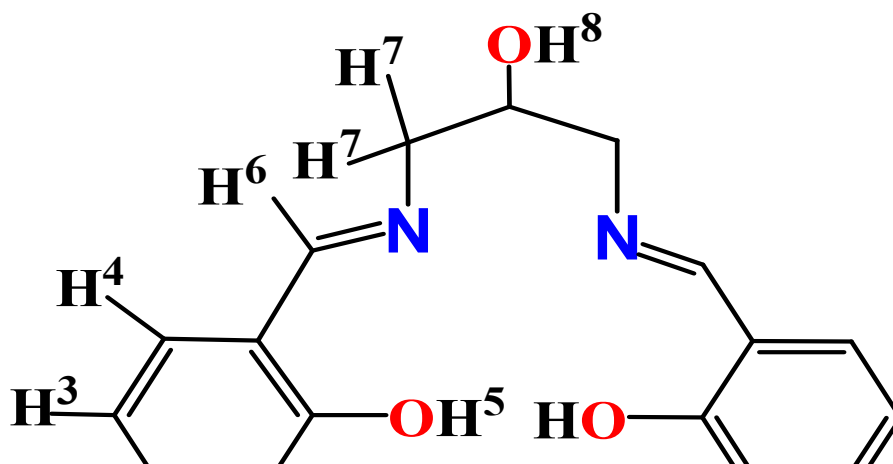
(M^I/M^{II}) facilitated the heteronuclear complex formation.



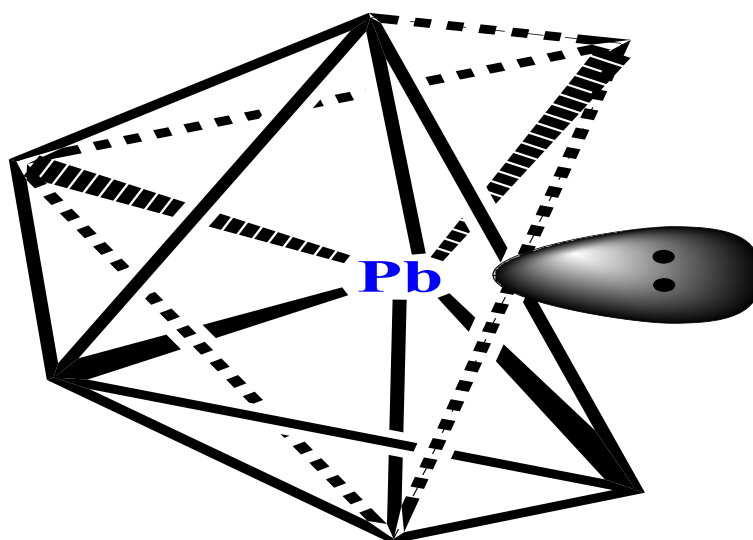
Scheme S2C. H₃L compartment occupancy by different metal ions (M¹/M²) facilitated the heteronuclear CP formation.



Scheme S3. The simplified Holo-directed and Hemi-directed coordination spheres around the Pb(II) metal ion.



Scheme S4. ^1H NMR Proton numbering Scheme of H_3L .



Scheme S5. Coordination polyhedral in $\text{Pb}(\text{II})$ complexes with donor ligands. For complexes with composition AX_6LP (CN A (6+LP)) the VSEPR model suggests the shape of a pentagonal bipyramid with the lone pair occupying the axial position or distorted octahedron geometry lone pair occupying capped position.

Table S1 Selected important bond distances (\AA) and Bond angles ($^\circ$) for the CP.

Bond distances (\AA)		
Pb1 S1 2.883(6)	Pb1 O2 2.420(6)	Pb1 O3 2.379(6)
Pb1 O1 2.710(7)	Pb1 O4 2.694(7)	Cd1 O2 2.235(6)
Cd1 O3 2.241(6)	Cd1 N3 2.12(8)	Cd1 N1 2.253(7)
Cd1 N2 2.253(8)		

Bond angles (°)			
O2 Pb1 S1 86.6(1)	O2 Pb1 O1 60.9(2)	O2 Pb1 O4 132.8(2)	O3 Pb1 S1 88.7(1)
O3 Pb1 O2 71.0(2)	O3 Pb1 O1 131.9(2)	O3 Pb1 O4 62.1(2)	O1 Pb1 S1 88.4(1)
O1 Pb1 O4 165.3(2)	O4 Pb1 S1 97.3(1)	O2 Cd1 O3 77.0(2)	O2 Cd1 N3 110.2(3)
O2 Cd1 N1 85.2(2)	O2 Cd1 N2 143.6(2)	O3 Cd1 N3 109.0(3)	N1 Cd1 O3 140.8(2)
N1 Cd1 N3 109.9(2)	N1 Cd1 N2 90.8(3)	N2 Cd1 O3 83.1(3)	N2 Cd1 N3 105.2(2)
Cd1 O3 Pb1 106.0(2)			

Table S2 Reported X-ray characterized Holo-/Hemi directed heteronuclear Pb(II) complexes.

Complexes	Coordination mode	Tetrel bonding	Ref
[Pb(OAc)(NiL ¹) ₂](OAc)	Holo-directed	Not explored	1

[NiL ² (H ₂ O) ₂ PbBr ₂]	Hemi-directed	Not explored	2
[NiL ² (H ₂ O) ₂ Pb(NO ₃) ₂]	√	Not explored	2
{L ³ Ni}Pb(NC ₅ H ₅)Cl] ₂	√	Not explored	3
[{L ⁴ Ni} ₂ Pb](H ₂ O)(Py)	√	Not explored	3
{[NiL ⁵ (py) ₂]PbCl ₂ }(Py)	√	Not explored	4
[NiL ⁶ Pb(NO ₃) ₂]	√	Not explored	5
[PbNiL ⁷ (AcO) ₂]	√	Not explored	6
[(H ₂ O)Ni(SCN)L ⁸ Pb(OAc)].DMSO	√	Present	7
[(H ₂ O) ₂ NiL ⁹ PbCl ₂]	√	Present	7
			7
[(SCN)NiL ⁹ Pb(NO ₃)]	√	Absent	7
[(H ₂ O)Ni(SCN)L ¹⁰ PbCl]	√	Absent	7
[(NCS)(H ₂ O)NiLPb(DMF)Cl]	No information	Not explored	8
[(SCN)NiL ¹ (μ _{1,3} -NCS)Pb]	No information	No explored	9
[(SCN)NiL ¹ (μ -OAc)Pb]			
[(SCN)NiL ² (μ -OAc)Pb]			
[{(DMSO)(H ₂ O)NiL ¹ } ₂ Pb](ClO ₄) ₂			
[{(DMSO)(H ₂ O)NiL ² } ₂ Pb](ClO ₄) ₂ ·4DMSO			
[(Cd)(Pb)(L)(η ¹ -NCS)(η ¹ -SCN)] _n (1)	Hemi-directed	Explored	This work

Table S3 Reported Covalent and Tetrel bond lengths (Å) in the structures of Pb(II) complexes.

Complexes	Bond lengths (Å)		Bond Nature	Ref
[PbL]ClO ₄] _n ·nH ₂ O	Pb-N	2.408(4)-2.513(4)	Covalent	10
		2.934(4)	Tetrel	
	Pb-O	2.382(4)	Covalent	

	ClO ₄ ⁻	3.201(5)	Tetrel	
{[Pb(HL)(OAc)]ClO ₄ } _n	Pb-N	2.612(6)-2.755(7)	Covalent	10
	Pb-O	2.572(5)-2.515(6)	Covalent	
	ClO ₄ ⁻	3.047(7)	Tetrel	
[PbL(NO ₂)] _n	ClO ₄ ⁻	3.309(10)	Tetrel	
	Pb-N	2.452(4)-2.837(3)	Covalent	10
		3.436(4)	Tetrel	
	Pb-O	2.384(5)-2.904(5)	Covalent	
[PbLN ₃] _n		3.299(4)	Tetrel	
	Pb-N	2.571(3)-2.837(3)	Covalent	10
		3.436(4)	Tetrel	
[Pb ₂ (HL) ₂ (NO ₃) ₂ (NCS) ₂]	N ₃ ⁻	2,321(3)-2.883(3)	Covalent	
	Pb-O	2.335(3)	Covalent	
	Pb-N	2.663(3)-2.460(4)	Covalent	10
	Pb-O	2.555(2)-2.882(2)	Covalent	
[PbL(OAc)] ₂	Pb-S NCS ⁻	3.2246(11)	Tetrel	
	Pb-N	2.490(3)-2.613(4)	Covalent	10
		3.030(4)-3.489(3)	Tetrel	
[(Cd)(Pb)(L)(η ¹ -NCS)(η ¹ SCN)] _n (1)	Pb-O	2.383(3)-2.753(4)	Covalent	
	Pb-N	2.697	Covalent	This work
	Pb-O	2.697(13)	Covalent	
	Pb-S SCN	3.337	Tetrel	

File Name C:\SAIF Kochi\Dhrubaj, WB\SA-13\0_B23\1

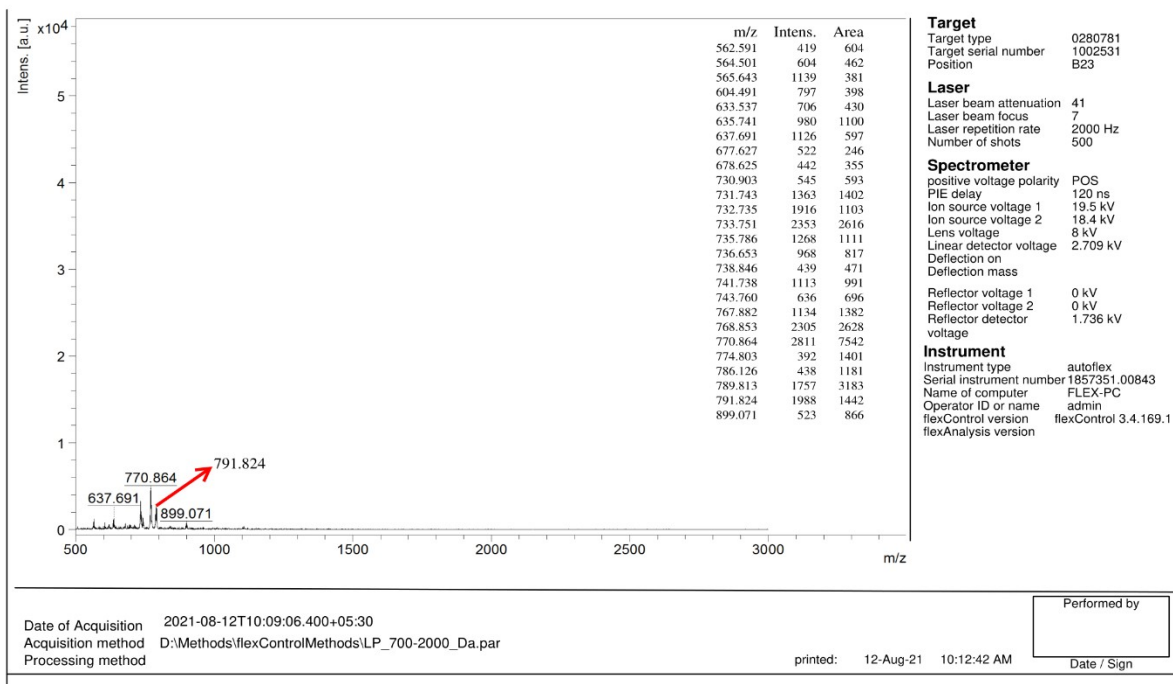


Fig.S1MALDI-TOF Mass of the CP.

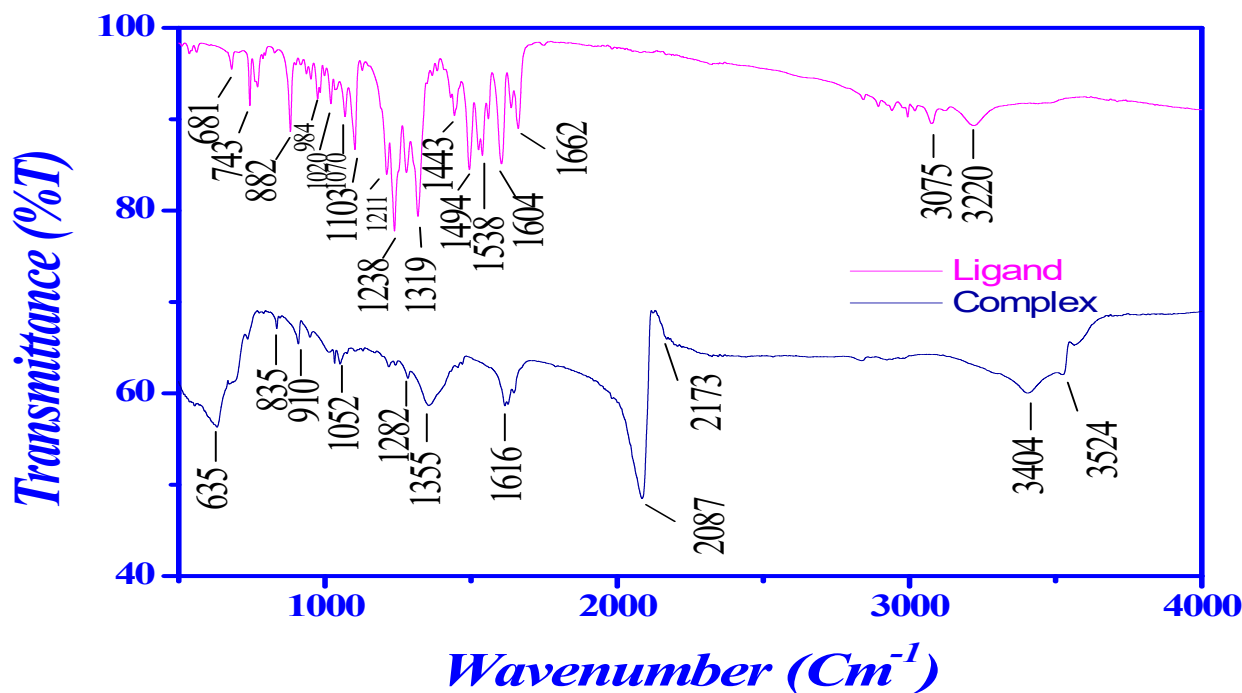


Fig.S1A Representative FT-IR spectra for Salen ligand and CP.

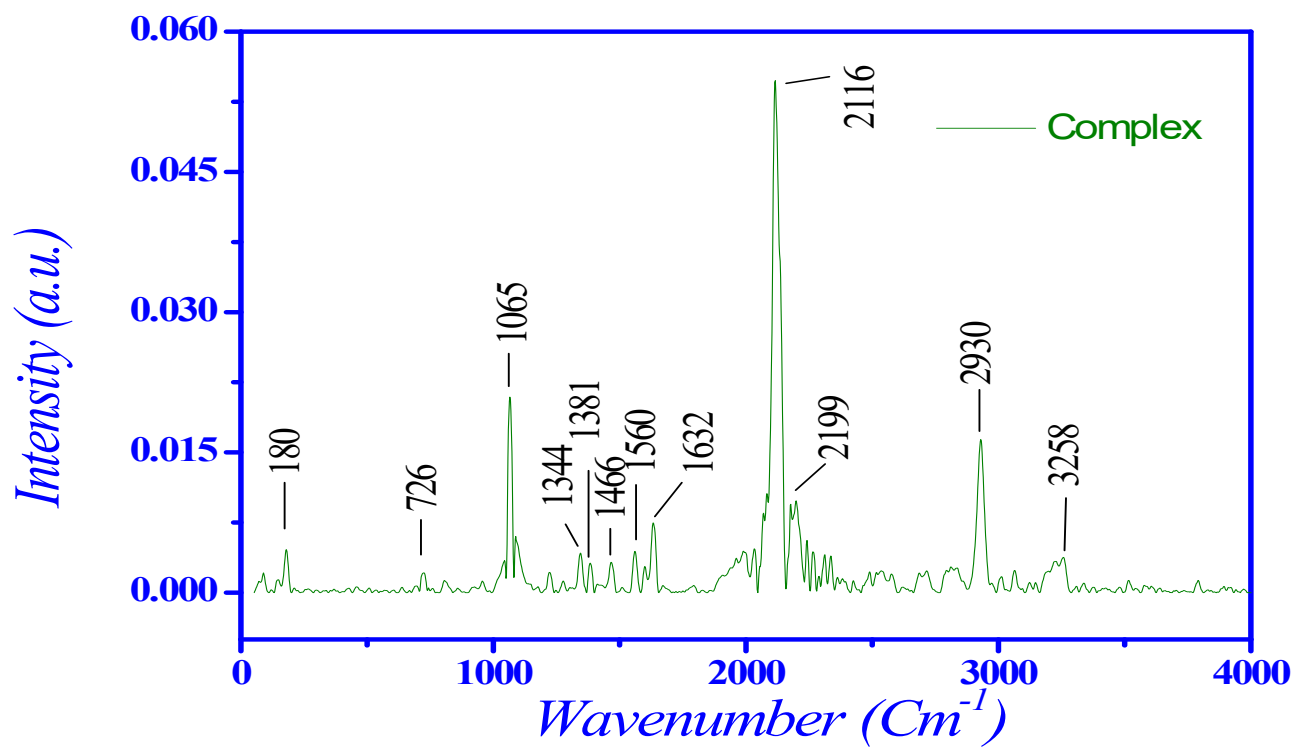


Fig.S2 Representative Raman spectra for the CP.

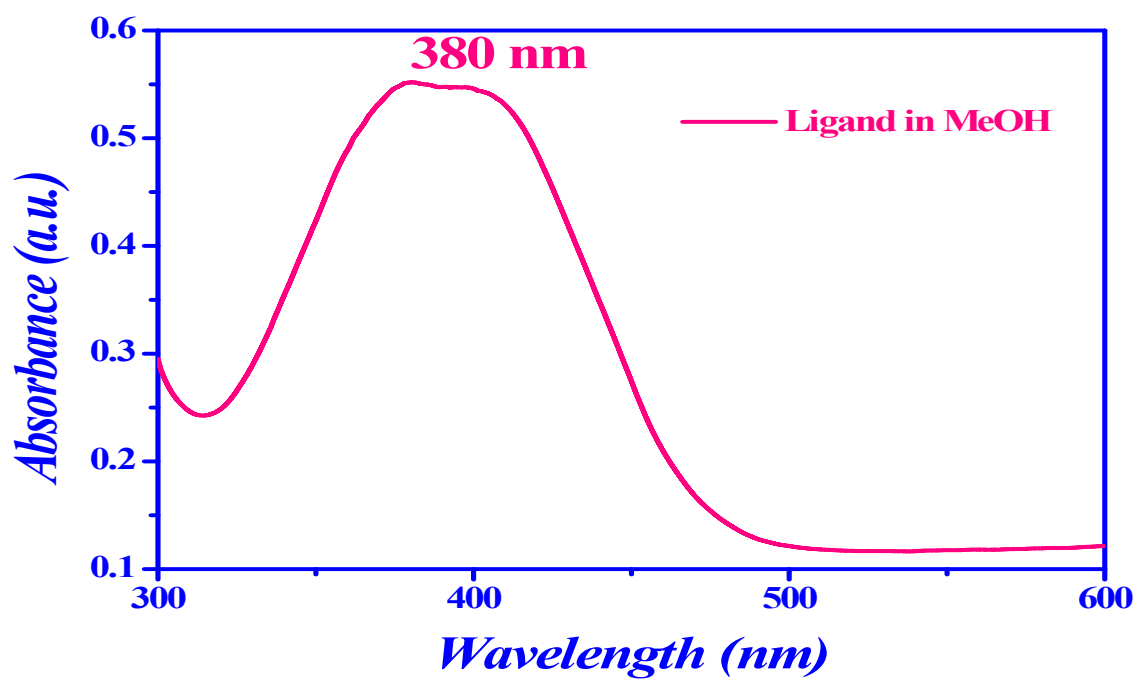


Fig.S3 Representative UV-Vis spectra for Ligand.

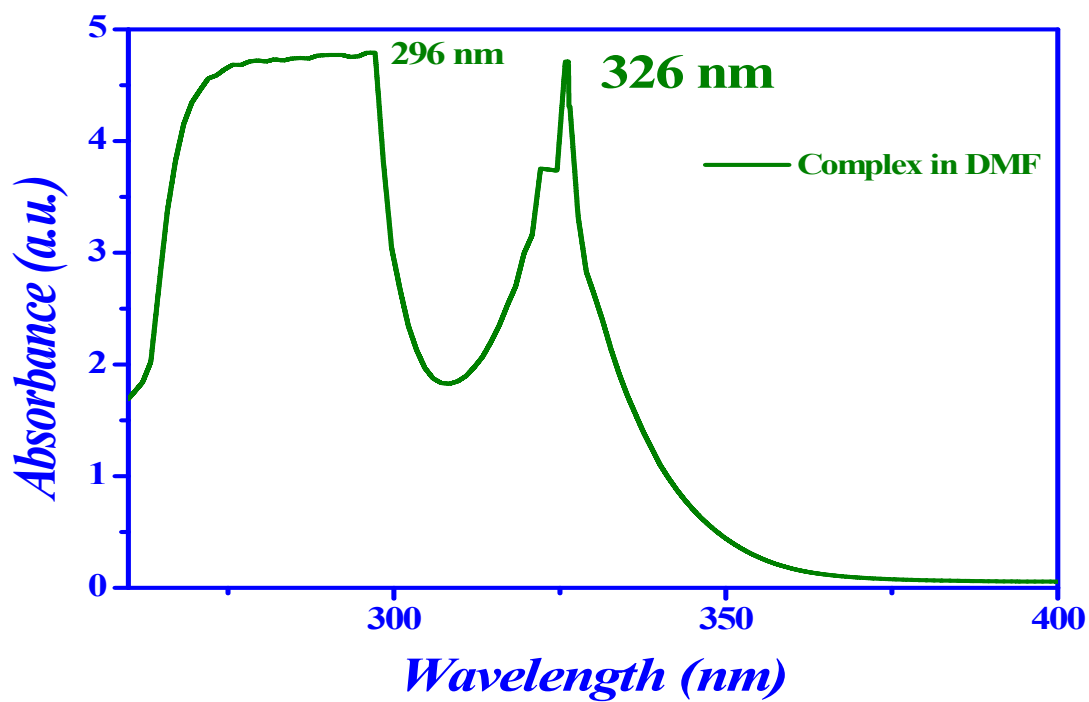


Fig.S4 Representative UV-Vis spectra for CP.

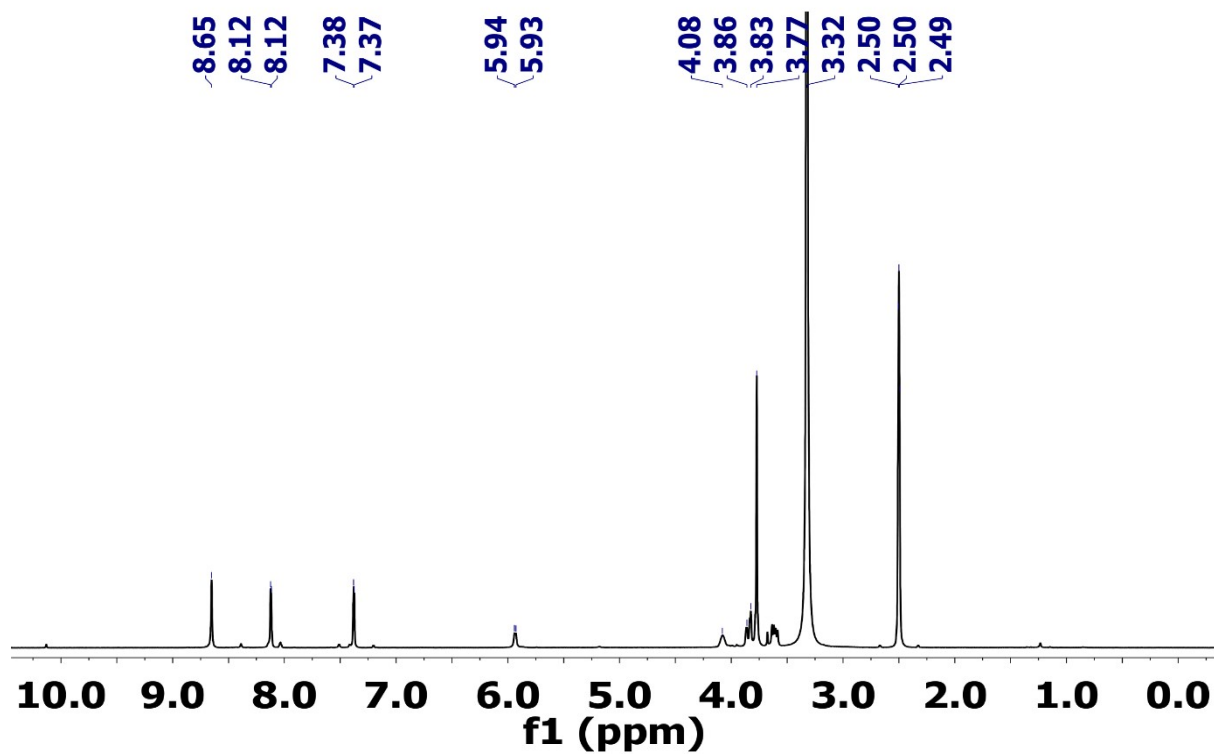
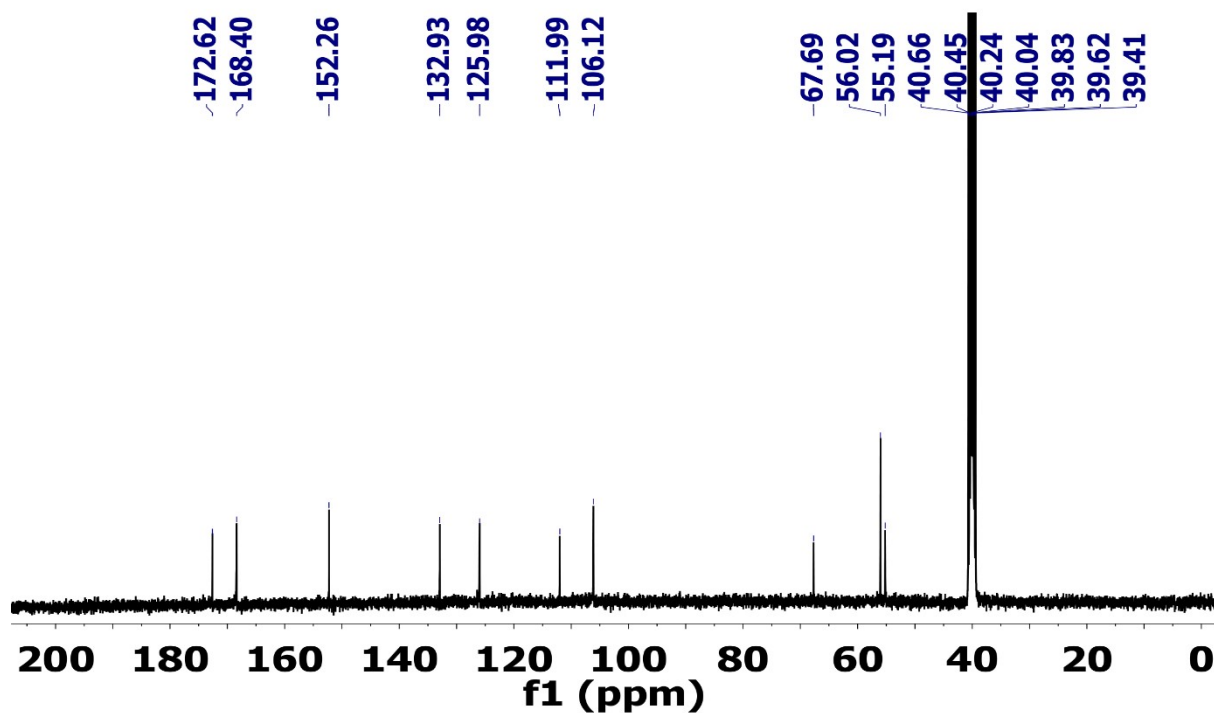
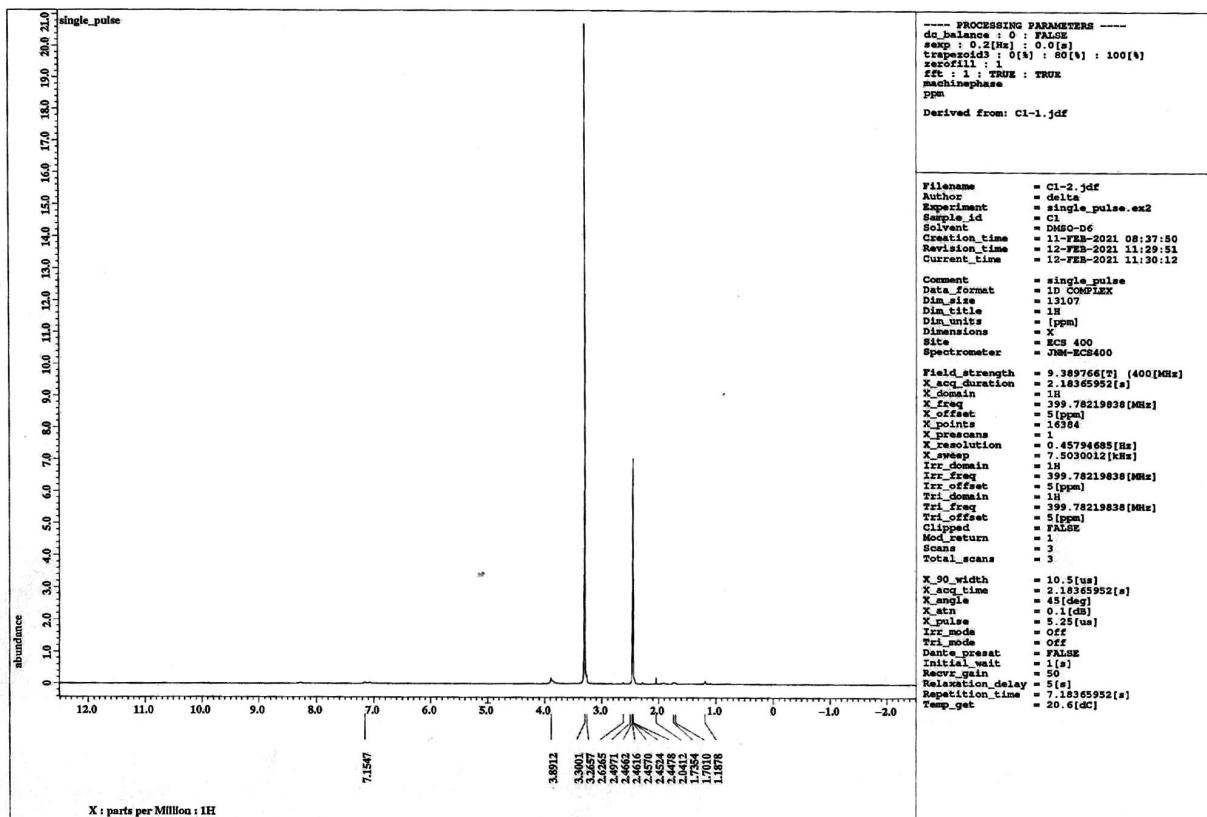


Fig.S5 Representative ¹H NMR spectra for Salen ligand.

Fig.S6 Representative ^{13}C NMR spectra for Salen ligand.Fig.S7 Representative ^1H NMR spectra for the CP.

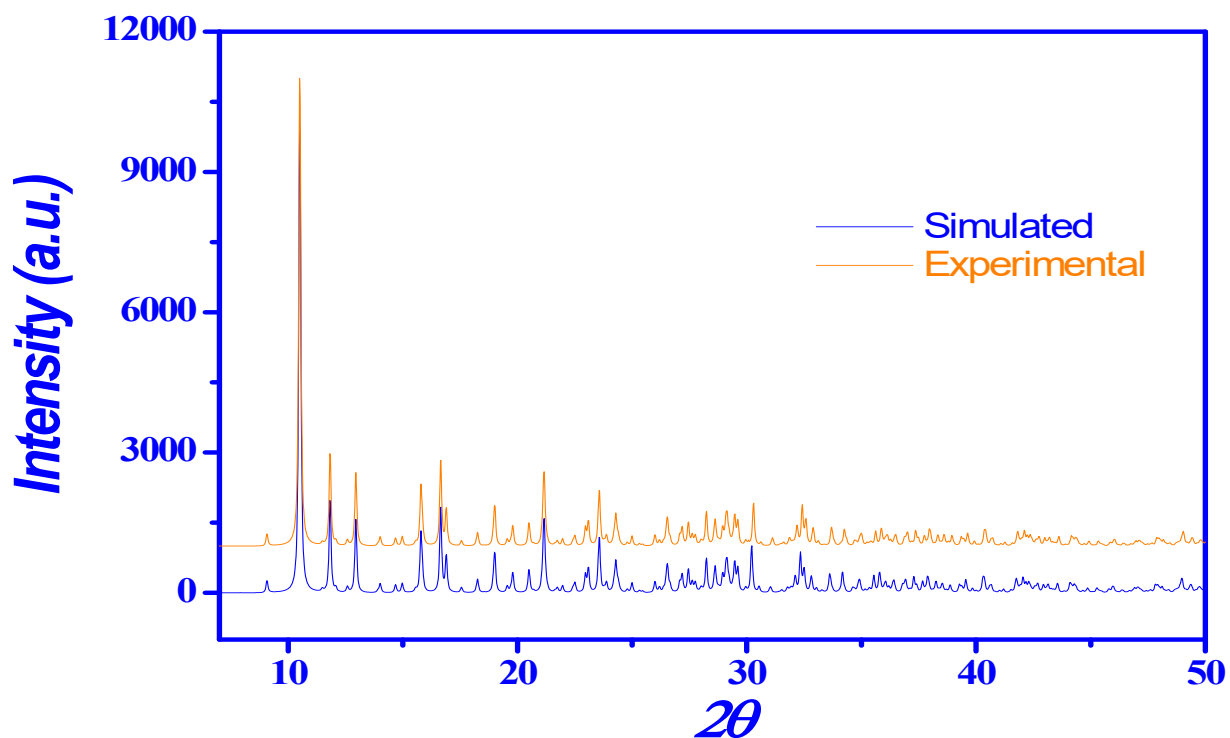


Fig.S8 Representative PXRD pattern for the CP.

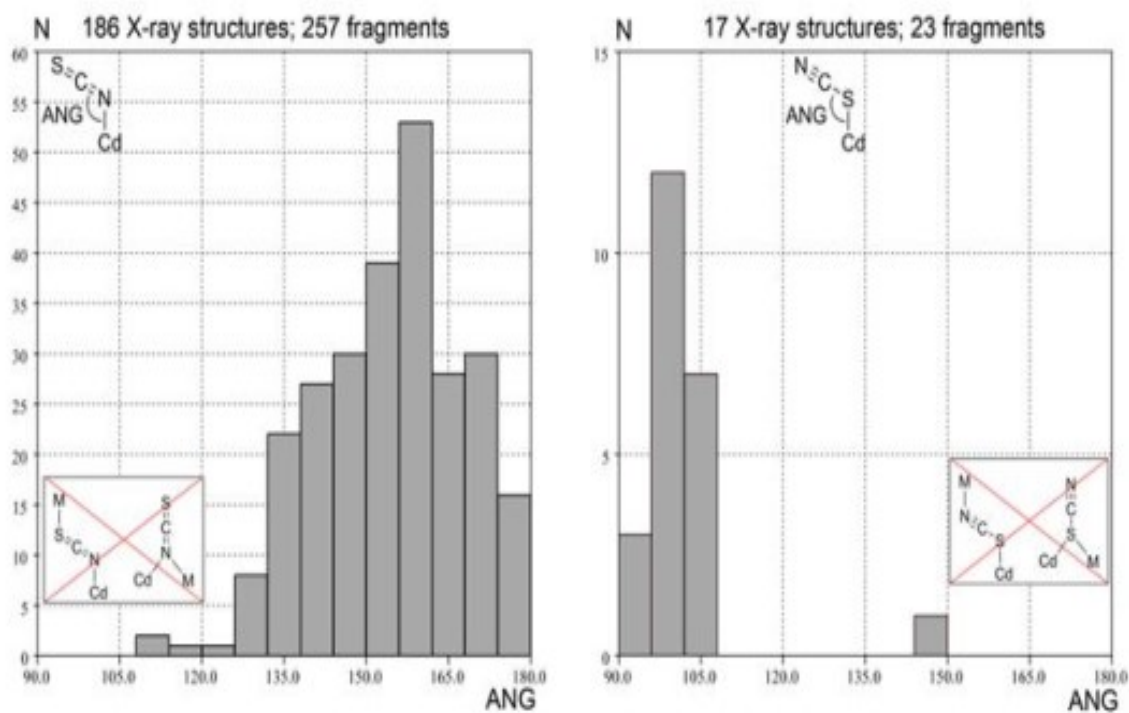


Fig.S9 Histogram plots of Cd-NC (left) and Cd-SC (right) angles in Cd-NCS and Cd-SCN complexes.

References

- 1 J. H. Thurston, C. G. -Z. Tang, D.W. Trahan, and K. H. Whitmire, *Inorg. Chem.*, 2004, **43**, 2708–2713.
- 2 S. Bhattacharya, and S. Mohanta, *Inorg. Chim. Acta.*, 2015, **432**, 169–175.
- 3 A. Mustapha, K. Busch, M. Patykiewicz, A. Apedaile, J. Reglinski, A. R. Kennedy, and T. J. Prior, *Polyhedron*, 2008, **27**, 868–878.
- 4 J. Reglinski, S. Morris, and D. E. Stevenson, *Polyhedron*, 2002, **21**, 2167-2174.
- 5 S. Sarkar, and S. Mohanta, *RSC Adv.* 2011.
- 6 K. -J. Inoue, M. Ohba, and H. Okawa, *BCSJ.*, 2002, **75**, 99–107.
- 7 S. Roy, M. G. B. Drew, A. Bauzá, A. Frontera, and S. Chattopadhyay, *New J. Chem.*, 2018, **42**, 6062–6076.
- 8 S. Roy, A. Dey, M. G. B. Drew, P. P. Ray, and S. Chattopadhyay, *New J. Chem.*, 2019, **43**, 5020–5031.
- 9 S. Mirdya, S. Roy, S. Chatterjee, A. Bauzá, A. Frontera, and S. Chattopadhyay, *Cryst. Growth Des.*, 2019, **19**, 5869–5881.
- 10 G. Mahmoudi, D. A. Safin, M. P. Mitoraj, M. Amini, M. Kubicki, T. Doert, F. Locherer, and M. Fleck, *Inorg. Chem. Front.*, 2017, **4**, 171–182.